

Superconducting energy gap in MgCNi₃ single crystals: Point-contact spectroscopy and specific-heat measurements

Z. Pribulová,¹ J. Kačmarčík,¹ C. Marcenat,² P. Szabó,¹ T. Klein,³ A. Demuer,⁴ P. Rodiere,³ D. J. Jang,⁵ H. S. Lee,⁵ H. G. Lee,⁶ S.-I. Lee,⁶ and P. Samuely¹

¹Centre of Very Low Temperature Physics at Institute of Experimental Physics, Slovak Academy of Sciences, Watsonova 47, 04001 Kosice, Slovakia

²CEA-Institut Nanosciences et Cryogénie/UJF-Grenoble 1, SPSMS, UMR-E 9001, LaTEQS, 17 rue des Martyrs, F-38054 Grenoble, France

³Institut Néel, CNRS and Université Joseph Fourier, Boite Postale 166, F-38042 Grenoble Cedex 9, France

⁴Grenoble High Magnetic Field Laboratory, CNRS, F-38042 Grenoble, France

⁵Department of Physics, Pohang University of Science and Technology, Pohang 790-784, Republic of Korea

⁶Department of Physics, National Creative Research Initiative Center for Superconductivity, Sogang University, Seoul 100-611, Republic of Korea

(Received 14 December 2010; revised manuscript received 26 January 2011; published 18 March 2011)

Specific heat has been measured down to 600 mK and up to 8 T by highly sensitive ac microcalorimetry on MgCNi₃ single crystals with $T_c \approx 7$ K. Exponential decay of the electronic specific heat at low temperatures proved that a superconducting energy gap is fully open on the whole Fermi surface, in agreement with our previous magnetic penetration depth measurements on the same crystals. The specific-heat data analysis shows consistently the strong-coupling strength $2\Delta/k_B T_c \approx 4$. This scenario is supported by the direct measurements of the gap via the point-contact spectroscopy. Moreover, the spectroscopy measurements show a decrease in the critical temperature at the sample surface, which accounts for the observed differences of the superfluid density deduced from the measurements by different techniques.

DOI: [10.1103/PhysRevB.83.104511](https://doi.org/10.1103/PhysRevB.83.104511)

PACS number(s): 74.25.Bt, 74.45.+c, 74.50.+r, 74.70.Ad

I. INTRODUCTION

The discovery of superconductivity in a cubic antiperovskite MgCNi₃ with the large ratio of Ni (60% in molar ratio) at about 8 K (Ref. 1) was a surprise, and it evoked a possible unconventional superconducting mechanism for which magnetic interactions may play an important role. Energy band calculations² have shown that the density of states at the Fermi level is dominated by Ni *d* states with a strong van Hove singularity yielding a narrow and strong peak in the density of states just below the Fermi energy. This type of narrow energy peak is typical for materials that display strong magnetic interactions. The peak was confirmed by x-ray spectroscopy experiments,^{3,4} but its spectral weight was largely suppressed compared with the theoretical predictions. Attempts to introduce a long-range magnetic order by increasing the density of states (DOS) via doping the Ni site have not been successful.⁵ Experimental indications of enhanced spin fluctuations in MgCN₃ have been found by nuclear-magnetic-resonance (NMR) investigations by Singer *et al.*⁶ together with isotropic *s*-wave superconductivity. Several papers have proposed a nonconventional (*d*-wave) superconducting order parameter based on the experimental findings of nonconventional critical current behavior⁷ and the zero-bias tunneling conductance.⁸ The penetration depth distinctly exhibited a non-BCS low-temperature behavior.⁹ The previous reports on the specific heat show conventional *s*-wave superconductivity with a phonon-mediated pairing mechanism.^{8,10–13} but at the same time an unusual low-temperature behavior was observed as well. The latter effect was attributed either to the Schottky contribution and/or the paramagnetism of unreacted impurities,^{8,10} or to an electron-paramagnon interaction in MgCNi₃ itself.^{12,13} Wälte *et al.*¹² have proposed

a two-band–two-gap model to account for different sizes of superconducting gaps found by different techniques. The anomalous point-contact Andreev-reflection spectra obtained by Shan *et al.*¹⁴ were interpreted using a model in which point contact made on a BCS superconductor is in series with the Josephson junction due to the polycrystalline character of the samples. To resolve this controversial situation, measurements on single crystals of good quality are highly desirable and have recently appeared.¹⁵ In our previous studies of magnetic penetration depth on those crystals,¹⁶ a fully open energy gap was found, in contrast to the results obtained on polycrystals. In our study, it was also found that the superfluid density extracted from the lower critical field was very different from that extracted from the tunnel diode oscillator measurements performed on the same sample. This discrepancy was related to the depletion of the critical temperature at the surface of the sample.

Here we present a detailed study of the high-quality MgCNi₃ single crystals by specific heat (C_p) and point-contact spectroscopy (PCS) measurements. One of the aims of this work has been to address the issue of differences that can appear between the bulk measurements (C_p) and surface measurements [PCS and previous penetration depth (λ) studies¹⁶]. That is why we used the same crystals or crystals from the same batches as those measured for λ . Exponential decay of the electronic specific heat at low temperatures confirmed that a superconducting energy gap is fully open on the whole Fermi surface, in agreement with our previous penetration depth measurements. The specific-heat data analysis shows consistently the strong-coupling strength $2\Delta/k_B T_c \approx 4$. This scenario is supported by the direct measurements of the gap via the PCS. Moreover, the PCS measurements show a decrease

in the critical temperature at the sample surface, accounting for the observed differences in the superfluid density deduced from the measurements by different techniques.

II. MEASUREMENTS

Recently, a long-standing problem of MgCNi_3 single-crystal preparation was overcome. The tiny samples were fabricated in a high-pressure closed system. Details of the synthesis can be found elsewhere.¹⁵ Using an x-ray microanalyzer, it was proven that carbon deficiencies in stoichiometry were negligible. However, in contrast to polycrystalline MgCNi_3 , which usually has local carbon deficiency, in these single crystals the Ni site was partly deficient. This was probably a reason for certain scattering in critical temperature among different crystals. T_c 's of our crystals as measured by specific heat were found between 6 and 7.5 K. Single crystals with a thickness of 0.1 mm have a rectangular shape and size of about $0.25 \times 0.15 \text{ mm}^2$.

Specific-heat measurements have been performed using an ac technique, as described elsewhere.^{17,18} ac calorimetry technique consists of applying periodically modulated sinusoidal power and measuring the resulting sinusoidal temperature response. In our case, an optical fiber is used to guide the heating power emitted from the diode toward the sample. The absence of a contact heater reduces the total addendum to the total specific heat. The temperature of the sample is recorded by a thermocouple. A precise *in situ* calibration of the thermocouple in magnetic field was obtained from measurements on ultrapure silicon. The magnetoresistance of the Cernox thermometer was precisely inspected, and corrections were included in the data treatment. Although an ac calorimetry is not capable of measuring the absolute values of the heat capacity, it is a very sensitive technique for measurements of relative changes on minute samples and enables one to carry out continuous measurements. We performed measurements at temperatures down to 0.6 K and in magnetic fields up to 8 T in the ^3He and ^4He refrigerators.

The PCS measurements were performed in the ^4He refrigerator. A standard lock-in technique was used to measure the differential resistance as a function of applied voltage on point contacts. The microconstrictions were prepared *in situ* by soft pressing of a mechanically formed platinum tip to the surface of the sample. The special approaching system enabled both the lateral and vertical positioning of the tip by the differential screw mechanism. Hence, our apparatus enables us to change the place where the tip touches the sample. Moreover, by regulating the tip pressure, it is possible to vary penetration of the tip into the sample surface.

III. RESULTS AND DISCUSSION

Figure 1 shows the temperature dependence of the total specific heat of the sample (plus addenda) in selected magnetic fields up to 8 T. The zero-field anomaly at the transition is very sharp ($\Delta T_c \approx 0.15 \text{ K}$), indicating the high quality and homogeneity of the single-crystal sample, much improved in comparison to polycrystals. The positions of the specific-heat jump gradually shift toward lower temperatures for increasing magnetic field. The anomaly remains well resolved at all

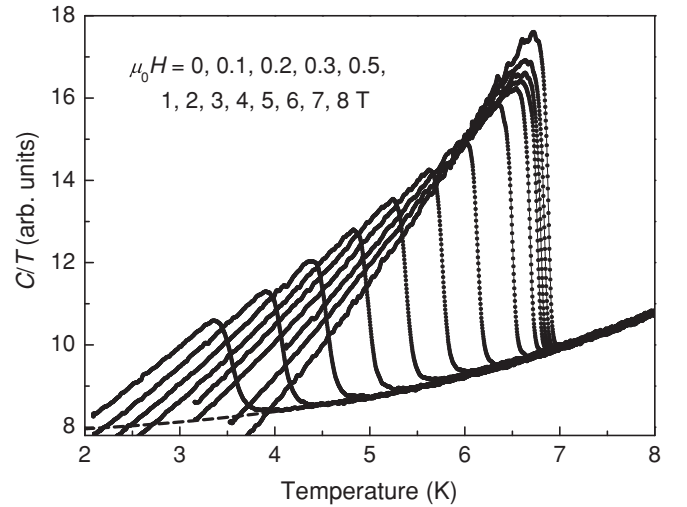


FIG. 1. Specific-heat anomaly measured in magnetic field. The zero-field measurement is the rightmost curve. Dashed line corresponds to the normal-state specific heat as calculated from the formula $C_n/T = a + bT^2 + cT^4$.

fields, showing only little broadening at high fields. Later we extended the measurements down to 0.6 K in a ^3He fridge, where the specific heat was measured at zero field and in 8 T. A field of 8 T was sufficient to completely suppress superconductivity down to about 4 K. The normal-state specific heat has been obtained from fits to the 8-T data between 4 and 12 K.

The normal-state specific heat of a nonmagnetic metal consists of the electronic specific heat $\gamma_n T$ with the Sommerfeld coefficient γ_n and the lattice part. At low temperatures, the lattice part is usually described by the Debye model $C_{\text{lattice}} = \beta T^3$. However, in the case of MgCNi_3 , the normal-state specific heat C_n shows a systematic deviation from this description. In some cases, as in Refs. 8 and 10, a strong low-temperature upturn of $C/T(T)$ is observed, indicating the presence of a Schottky anomaly probably due to magnetic impurities. In the case of the polycrystalline samples of Wälte *et al.*¹² and Shan *et al.*,¹³ the deviations are much smaller and could be described either by a higher phonon term ($\sim T^5$) or by additional electron-paramagnon interaction. In our case, C_n could also be fitted with $C_n = aT + bT^3 + cT^5$. Our C_n comprises inevitably also the addenda, but since all known specific-heat measurements on MgCNi_3 so far, independently of the form of the sample (polycrystals or single crystals) and the method of measurements, show the presence of a low-temperature upturn, we believe it is intrinsic. We attribute it to the higher-phonon term. This interpretation is supported by experimental observation of the softening of the lowest acoustic Ni phonon modes below 200 K by Heid *et al.*¹⁹ But our measurements cannot exclude a paramagnon contribution as well.

To derive the electronic specific heat, we first subtracted the normal state specific heat C_n , i.e., we calculated $\Delta C(T)/T = C(T)/T - C_n(T)/T$. By doing so, we eliminate the addenda and phonon (eventually paramagnon) contribution. Figure 2 represents the resulting temperature dependence of $\Delta C/T$. The transition temperature obtained from entropy balance

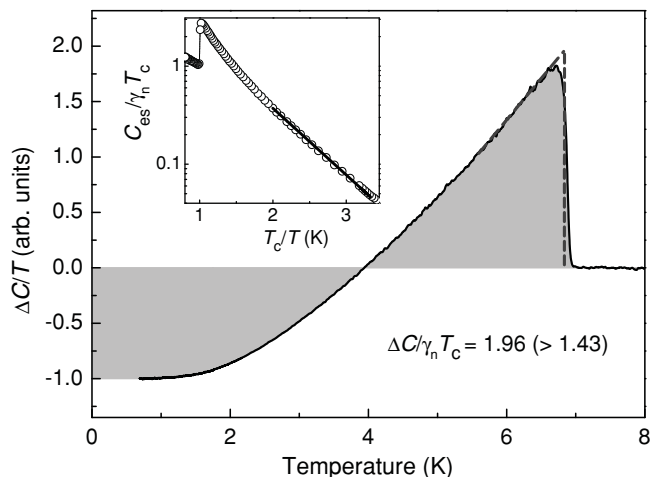


FIG. 2. Temperature dependence of specific heat in zero magnetic field. Dashed line is entropy conservation construction around critical temperature. Inset: exponential dependence of the electronic specific heat; full line represents the best fit of the exponential decay.

construction around the anomaly (vertical dashed line in Fig. 2) is $T_c = 6.85$ K. The entropy conservation required for a second-order phase transition is fulfilled, as indicated by the hatched areas in Fig. 2 (see also the inset in Fig. 3). This check supports the determination of the normal state specific heat and it verifies the thermodynamic consistency of the data. By the balance of entropy around the transition, the dimensionless specific-heat jump $\Delta C/\gamma_n T_c = 1.96$ at T_c is determined, where $\gamma_n = \frac{C_p}{T}|_{0.6\text{K}} - \frac{C(H=0)}{T}|_{0.6\text{K}}$. $\Delta C/\gamma_n T_c$ is an important measure of the electron coupling, which is significantly stronger here than in the BCS weak-coupling limit equal to 1.43.

To further estimate the coupling strength, we compared the electronic specific heat $C_{es}/T = \Delta C/T + \gamma_n$ of MgCNi₃ with the so-called α model²⁰ based on the BCS theory. In this model, the only adjustable parameter is the gap ratio $2\Delta/k_B T_c$. Our data could be well described by the model with a ratio $2\Delta/k_B T_c \approx 4.2$, which is much higher than the canonical value of 3.52 for the BCS superconductor.

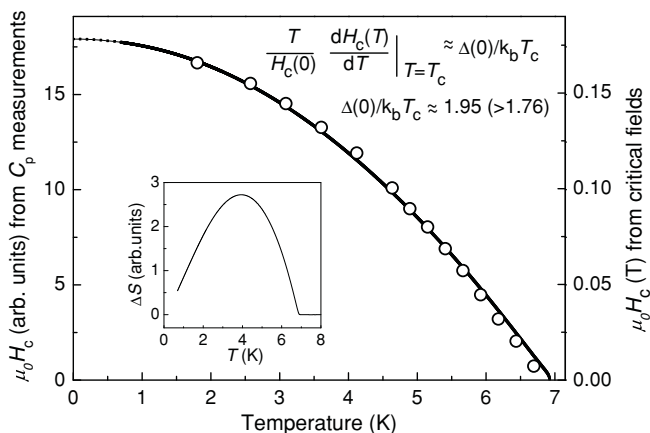


FIG. 3. Temperature dependence of thermodynamic critical field as derived from electronic specific heat (line), left axis applies. Right axis applies to the $\mu_0 H_c(T)$ as calculated from H_{c1} found in Ref. 16 and H_{c2} from Fig. 4 (circles); see text for details. Inset: Difference of entropy between normal and superconducting state.

The inset of Fig. 2 displays the logarithm of C_{es} versus T_c/T . As shown, one obtains an exponential dependence $C_{es} \propto c_1 \exp(-c_2 T_c/T)$ for $T_c/T \geq 2$. This is strong evidence that a full gap is present on the whole Fermi surface of MgCNi₃ and is in full agreement with our previous penetration depth measurements¹⁶ on the same crystal. Exponential decay of the low-temperature specific heat contradicts the presence of any nonconventional order parameter in the system. The solid line in the inset represents the best fit of the data in the temperature range 2–3.5 K. The data could well be fitted by the expression $8.5 \exp(-1.57T/T_c)$, which shows an exponent higher than in the BCS prediction $8.5 \exp(-1.44T/T_c)$ valid for this temperature range. This leads to the strong-coupling ratio of $2\Delta/k_B T_c \sim 3.84$. The exponent 1.57 found in our experiment is even slightly higher than the value of 1.53 found by Wälte *et al.*¹²

The thermodynamic critical field $H_c(T)$ contains also information about the coupling strength in the superconductor. H_c can be determined from the electronic specific heat by double integration of the data. First of all, we calculate the difference of entropy between the superconducting and the normal state as $\Delta S(T') = \int_{T'}^{T_c} (\Delta C/T) dT$, i.e., the integral of the data from Fig. 2. Then, we get the thermodynamic critical field as $H_c^2(T'') = 8\pi \int_{T''}^{T_c} \Delta S(T') dT'$, i.e., from the second integration. Figure 3 shows the resulting temperature dependence of H_c (line). The inset represents the difference of entropy between the superconducting and the normal state in MgCNi₃ calculated as explained above. Since the results of ac calorimetry measurements are in arbitrary units, such calculated H_c is also in arbitrary units. Yet we can determine the ratio $[T/H_c(0)](dH_c/dT)|_{T=T_c}$, which is close to $\Delta(0)/k_B T_c$.²¹ Taking the value of $\mu_0 H_c(0) = 17.9$ and derivative of H_c in the vicinity of T_c equal to 5.1, we get the coupling ratio $2\Delta/k_B T_c = 3.9$, well in agreement with our previous estimates.

To prove the consistency of our data, we compared H_c calculated from the specific heat with those calculated from the lower and upper critical fields (H_{c1} and H_{c2} , respectively) as $\mu_0 H_c = \mu_0 \sqrt{H_{c1} H_{c2}} / (\ln \kappa + 0.5)$, where the Ginzburg-Landau parameter κ was determined from H_{c1} and H_{c2} as described in Ref. 22. The temperature dependence of H_{c1} was taken from our previous work,¹⁶ and the values of H_{c2} are from Fig. 4 of this work. The resulting $\mu_0 H_c(T)$, now in absolute units, is displayed in Fig. 3 by circles for which the right axis applies. The data are in excellent agreement with those calculated by the double integration of the electronic specific heat. With the zero-temperature coherence length $\xi(0) = 5.24$ nm determined from the upper critical field ($\xi = \sqrt{\Phi_0/2\pi\mu_0 H_{c2}}$ with the flux quantum Φ_0) and $\lambda(0) = 230$ nm,¹⁶ we get the Ginzburg-Landau parameter $\kappa(0) = 44$. All obtained critical parameters ($T_c, H_{c2}(0), H_{c1}(0), H_c(0)$) as well as the zero-temperature coherence and penetration lengths are in very good agreement with those determined by Wälte *et al.*¹² from the specific-heat measurements on polycrystalline samples.

We have done the equivalent specific-heat measurements and the data analysis on several other crystals with $T_c = 6$ and 7.5 K. We found very similar results concerning the height of the specific-heat jump $\Delta C(T_c)/\gamma_n T_c$, which was close to 2, as

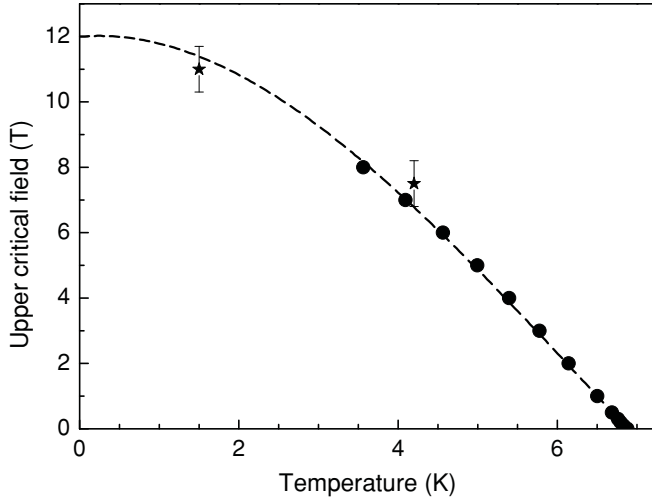


FIG. 4. Temperature dependence of the upper critical field in MgCNi₃ from specific-heat measurements (circles) and point-contact spectroscopy (stars). Dashed line is corresponding temperature dependence of H_{c2} from WHH theory.

well as the value of coupling strength $2\Delta/k_B T_c$, which was close to 4.

Figure 4 shows the upper critical field in MgCNi₃ derived from the specific-heat measurements in magnetic field presented in Fig. 1. The midpoint of the transitions has been taken as a criterion to determine H_{c2} for each magnetic-field measurement. The temperature dependence of H_{c2} reveals a linear increase close to the critical temperature and gradual deviation from linearity at lower temperatures as measured down to 3.5 K. Though measured only down to $T_c/2$, $H_{c2}(T)$ can be satisfactorily described in the framework of the Werthamer-Helfand-Hohenberg (WHH) theory,²³ as indicated by the dashed line in Fig. 4. WHH predicts that $H_{c2}(0) = 0.693T_c(dH_{c2}/dT)_{T_c}$. With the slope $\mu_0(dH_{c2}/dT)_{T_c} = 2.5$ T/K, we get $\mu_0 H_{c2}(0) = 12$ T. Two points in Fig. 4 obtained from the point-contact spectroscopy measurements (see below) support this agreement even better. The Clogston paramagnetic critical field is the upper limit of the superconductivity at low temperature and is given as $H_p(0) = \frac{1}{\sqrt{2}\mu_B} \Delta$,²⁴ where μ_B is the Bohr magneton. For our strong-coupling case (with $2\Delta/k_B T_c = 3.9$), $\mu_0 H_p(0) = 14$ T is quite close to the observed values.

One can calculate the Fermi velocity as $v_F = \pi \Delta \xi / \hbar = 3 \times 10^4$ m/s (with our $\Delta = 1.15$ meV as determined above). This can be compared with the band-structure calculations of the Fermi velocities in the hole and electron subsystems in MgCNi₃.¹² The calculated hole Fermi velocity is $v_{F,h} = 12 \times 10^4$ m/s and the electron velocity is $v_{F,e} = 50 \times 10^4$ m/s. For $H_{c2}(0)$, the slower Fermi velocity will play a dominant role, and this is the hole one. In any case, our calculated value is at least four times smaller. This difference can be attributed to the strong electron-phonon renormalization factor $(1 + \lambda_{e-ph})$. As introduced by McMillan and Werthamer²⁵ and further elaborated by Shulga and Drechsler,²⁶ the strong-coupling corrections lead to the modified upper critical field as $H_{c2}^M(T) = H_{c2}(T)(1 + \lambda_{e-ph})^n$, where $n \geq 2$. A very strong electron-phonon coupling constant $\lambda_{e-ph} \geq 2$ is then needed

to explain the differences in the above-mentioned Fermi velocities. As indicated in Ref. 12, such a strong coupling would require a sizable depairing contribution to explain the low T_c in MgCNi₃. One possible mechanism may be the existence of important electron-paramagnon interaction in the system, as suggested in Refs. 13 and 12.

Note, however, that a significant increase of the H_{c2} value might also be induced by scattering effects in the so-called dirty limit, in which case H_{c2} becomes proportional to $1/(\xi l)$, where l is the electronic mean free path (see the discussion in Ref. 12). Typically, our single crystals have a residual resistivity $\rho \approx 23 \mu\Omega$ cm.²⁷ By evaluating the unrenormalized mean free path $l = \frac{\langle v_F \rangle}{\epsilon_0 \rho \omega_p^2}$, with $\langle v_F \rangle$ the average Fermi velocity [2.1×10^5 ms⁻¹ (Ref. 12)] and ω_p the plasma frequency [3.17 eV (Ref. 12)], one gets a mean free path of a few nm, suggesting the sample may be in or close to the dirty limit.

Finally, a very large difference between the Fermi velocity deduced from band-structure calculations and the one deduced from the upper critical field has also been obtained recently in Fe(Se,Te) (Ref. 28) (reaching in this case a factor of ~ 20). In this later system, this difference has been attributed to strong correlation effects in the normal states (see also Ref. 29). To the best of our knowledge, the role of correlations has not been addressed so far in MgCNi₃. Note that both MgCNi₃ and Fe(Se,Te) share the similarity of having Fermi surfaces composed of both electron and holes pockets (3D sheets in MgCNi₃ instead of quasi-2D ones in iron-based superconductors), and both systems are subjected to strong spin fluctuations. However, it is generally assumed that those fluctuations lead to opposite effects in each system, being at the origin of the pairing mechanism in the so-called $s \pm$ model in iron-based systems but strongly reducing the electron-phonon coupling constant in MgCNi₃. We show here that both systems also have very strong critical field [being close to the Pauli limit in MgCNi₃ and even limited by this Pauli field on a large part of the H - T diagram in Fe(Se,Te)], and the similarity between those two systems probably deserves further study.

The point-contact spectra have been measured mostly on a bigger crystal of MgCNi₃ with a size of approximately $0.4 \times 0.2 \times 0.1$ mm³, but some measurements were also done on the same crystal as used for the specific-heat measurements with $T_c = 6.85$ K. T_c of the bigger crystal was 6.7 K, as determined locally by point-contact spectroscopy. The experimental differential conductance curves have revealed the typical characteristics of a single-gap superconductor with a single pair of gaplike peaks. The measured point-contact spectra were normalized to the conductance background found at higher energies above the superconducting gap. This allowed for fits of the conductances to the point-contact model of Blonder, Tinkham, and Klapwijk (BTK), accounting also for the spectral broadening³⁰ and to get information about the energy gap Δ , a parameter of the barrier strength Z , and a spectral broadening Γ . The barrier strength Z was affected by adjustable pressure of the tip on the sample. Low-pressure junctions have yielded more tunneling characteristics with the barrier parameters $Z \approx 0.6 - 1$, while more Andreev-reflection characteristics with $Z < 0.6$ were found when the pressure was increased. The latter contacts revealed a value of the gap scattered between 1.1 and 1.2 meV. Taking into

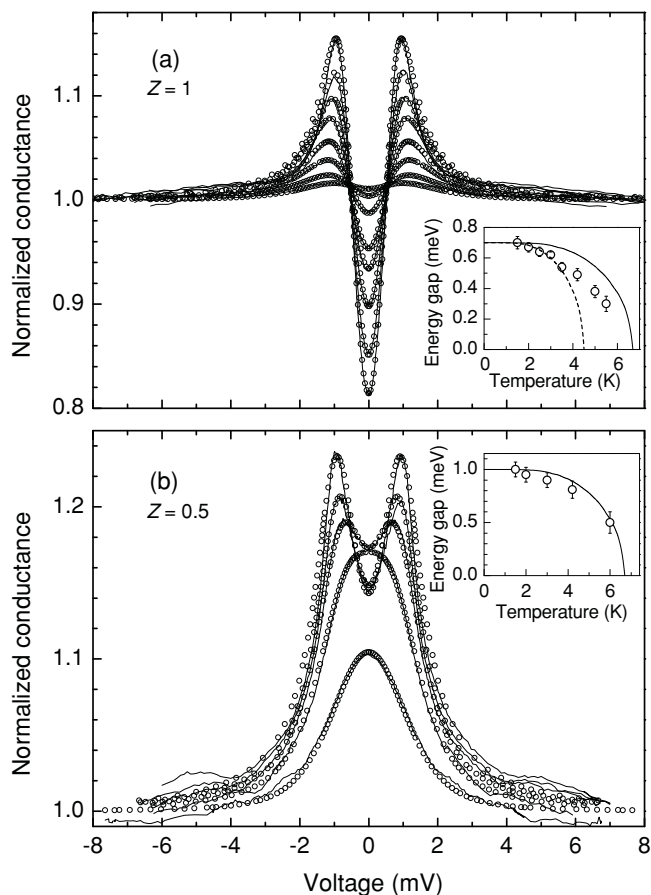


FIG. 5. (a) Pt-MgCNi₃ point-contact spectra (solid lines) measured at 1.5, 2, 2.5, 3, 3.5, 4.2, 5, and 5.5 K and fitting curves (open symbols). Inset: temperature dependence of energy gaps from fits to the spectra in the main figure (open symbols) and BCS-like temperature dependences displayed by solid and dashed line for two different T_c 's. (b) Point-contact spectra of another junction (solid lines) measured at 1.5, 2, 3, 4.2, and 6 K with fitting curves (open symbols). Inset: temperature dependence of fitted energy gaps (open symbols) and BCS-like temperature dependence.

account $T_c \sim 6.7$ K, we obtain the coupling ratio of $2\Delta/kT_c \sim 3.8$ – 4.2 . In some measurements on the junctions with more tunneling-like characteristics, we have found the energy gap value at much smaller energies of around 0.7 meV.

In order to perform more precise analysis, some point contacts have been measured at different temperatures. Figure 5(a) displays the point-contact spectrum with a smaller gap (solid lines). The symbols represent the best fit to the BTK model at each particular temperature. Fitting parameters Γ and Z were first obtained for the spectrum at 1.5 K and then kept constant when fitting the curves measured at higher temperatures. From the fit we found the superconducting gap $\Delta = 0.7$ meV at 1.5 K, with Γ being on the order of 40% of Δ and $Z \sim 1$. The inset shows the temperature dependence of this energy gap (open symbols). Surprisingly, the data display a strong deviation from the BCS-type of temperature dependence with $\Delta(0)$ as a free parameter (solid line). Taking into account the local critical temperature of the contact $T_c \sim 6.7$ K, one obtains the coupling ratio $2\Delta/kT_c \sim 2.5$. This value is much lower than the canonical BCS

weak-coupling value of 3.52. Such a low value of the energy gap was also obtained on some point contacts measured by Shan *et al.*¹⁴ on polycrystalline MgCNi₃. The fact that both a low-energy gap and deviations from a typical BCS temperature dependence have been observed on low-pressure contacts indicates that a degraded superconductivity on the surface of the sample has been at play. The degraded layer may have smaller T_c than the bulk, and the energy gap could reveal a tendency to close at lower temperatures than the bulk T_c , as is indicated by the dashed line in the inset, yielding the surface critical temperature of 4.5 K and the corresponding coupling constant of $2\Delta/kT_c \sim 3.5$. The point contact probes the superconductivity at a distance of the coherence length from the junction. At increased temperatures, the coherence length increases and adjacent layers deeper in the superconducting bulk with a higher T_c will be probed. As a result, the measured gap does not follow the dashed line, but it shows a finite value up to the bulk T_c of 6.7 K.

Figure 5(b) shows the spectra of another point contact (lines), now with a lower barrier strength, together with the fits at the selected temperatures (symbols). The fitting parameters $\Delta(1.5 \text{ K}) = 1$ meV, $\Gamma = 0.4$ meV, and $Z \sim 0.5$ are found. The inset displays the temperature dependence of this energy gap (symbols). Comparison with the BCS-like curve (line) shows that despite the fact that the ratio $2\Delta/kT_c$ for this contact is close to 3.52, there is still a deviation similar to, though smaller than, that in the previous case. This indicates that even the value of $\Delta(0) = 1$ meV is an underestimate of the bulk energy gap³¹ and that the value of 1.1–1.2 meV found on other junctions is closer to the one related to the bulk phase with $T_c = 6.7$ K. Thus, the coupling ratio of $2\Delta/kT_c \sim 4.0$ is suggested by our point-contact spectroscopy measurements, which is in reasonable agreement with the value determined from the specific heat.

In previous measurements,¹⁶ we have observed a drastically different behavior between the superfluid density at low temperatures extracted from the Hall probe and tunnel diode oscillator (TDO) measurements performed on the same crystal of MgCNi₃. On the other hand, the difference has been vanishing near the common T_c . At low temperatures, TDO measurements probe only the sample surface, while measurements by the Hall probe are sensitive to the bulk of the sample. Among the possible explanations, a systematic decrease in the critical temperature at the sample surface has been suggested. Lower T_c at the surface would cause a higher penetration depth that enters into the expression for superfluid density. We have estimated that 20% lower T_c at the surface could explain the observed difference in superfluid density. The difference in T_c 's indicated by the dashed and solid lines related to the small gap of $\Delta(0) = 0.7$ meV [inset of Fig. 5(a)] is very close to this estimation, supporting the explanation with a degraded superconductivity on the sample's surface.

Figure 6 shows the normalized conductance spectrum of another point contact measured at 1.5 K at various magnetic fields. Apparently, the presented junction reveals quite a significant contribution from the direct conductance, which is supported by the fit giving $Z \sim 0.3$. The spectrum is very broadened, with $\Gamma \sim 1.1$ meV on the order of the value of the energy gap, and the broadening is also responsible for a low intensity of the spectrum. Nevertheless, such a junction

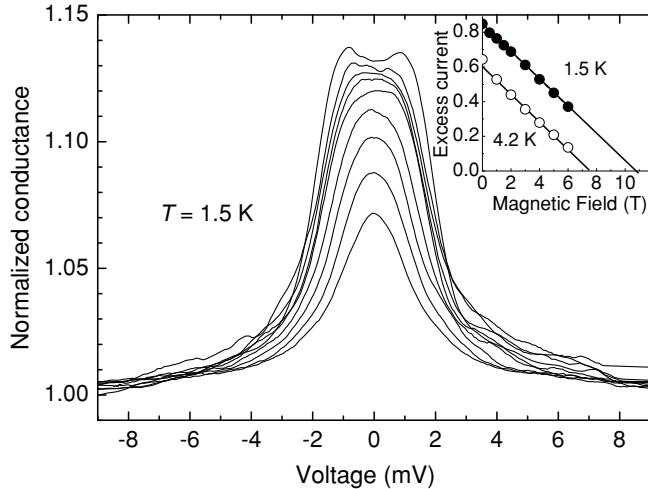


FIG. 6. Pt-MgCNi₃ point-contact spectra measured at 1.5 K in magnetic fields of 0 (topmost curve), 0.5, 1, 1.5, 2, 3, 4, 5, and 6 T. Inset: Determination of the upper critical field from magnetic-field dependence of excess current.

with a low barrier strength Z can be used to determine the excess current, which can be approximated as the value of the area between the normalized conductance spectrum and unity: $I_{\text{exc}} \approx \int (\frac{dI}{dV} - 1)dV$. The magnetic-field dependences of I_{exc} for 1.5 and 4.2 K of the junction are shown in the inset. In both cases, I_{exc} decreases linearly with increasing magnetic field. A suppression of the excess current with increasing magnetic field is associated with the increasing number of vortices, with cores representing a normal state area in the point contact. At the upper critical field $H_{c2}(T)$ at the normal state, the excess current vanishes. By extrapolating $I_{\text{exc}} \rightarrow 0$, the upper critical fields $\mu_0 H_{c2}$ are found at 4.2 and 1.5 K. They are shown by stars in Fig. 4. $\mu_0 H_{c2}(4.2 \text{ K})$ is in good agreement with the specific-heat determination, and $\mu_0 H_{c2}(1.5 \text{ K})$ expands the experimental data to the lowest temperatures and proves the WHH type of temperature dependence. Importantly, the overall temperature dependence of the upper critical field is in perfect quantitative agreement with the determinations from transport measurements done on the crystals from the same batch.²⁷

It is worth noticing that the magnetic-field dependence of the excess current obtained on the MgCNi₃ point contact behaves very differently from the case of MgB₂, a spectacular two-gap superconductor, where it decreases with two different subsequent slopes in accordance with different filling rates of the two gaps.³² Then, the linear decrease of $I_{\text{exc}}(H)$ proves independently the presence of a single gap in the excitation spectrum of MgCNi₃.

IV. CONCLUSIONS

Specific-heat data obtained by ac calorimetry show a sharp and well-resolved superconducting transition in magnetic fields up to 8 T. The results confirm the very high quality of our MgCNi₃ single crystals used in the study. The low-temperature electronic specific heat clearly reveals an exponential decrease—strong evidence for s -wave superconductivity that is in a very good agreement with the previous penetration depth measurement on the same crystals. The ratio $2\Delta/k_B T_c \approx 4$ and high specific-heat jump at the transition in zero field, $\Delta C(T_c)/\gamma_n T_c \approx 1.96$, confirmed the presence of strong-coupling superconductivity in the system. This scenario is supported by the direct gap measurements via the point-contact spectroscopy. Moreover, the spectroscopy measurements show a decrease in the critical temperature at the sample surface, which accounts for the observed differences of the superfluid density deduced from the measurements by different techniques.

ACKNOWLEDGMENTS

This work was supported by the EC Framework Programme MTKD-CT-2005-030002, by the EU ERDF (European regional development fund), Grant No. ITMS26220120005, by the Slovak Research and Development Agency, under Grants No. VVCE-0058-07, No. APVV-0346-07, No. SK-FR-0024-09, and No. LPP-0101-06, and by the US Steel Kosice, s.r.o. The Centre of Low Temperature Physics is operated as the Centre of Excellence of the Slovak Academy of Sciences. We thank G. Karapetrov for a careful reading of the manuscript.

¹T. He, Q. Huang, A. P. Ramirez, Y. Wang, K. A. Regan, N. Rogado, M. A. Hayward, M. K. Haas, J. S. Slusky, K. Inumara, H. W. Zandbergen, N. P. Ong, and R. J. Cava, *Nature (London)* **411**, 54 (2001).

²D. J. Singh and I. I. Mazin, *Phys. Rev. B* **64**, 140507(R) (2001).

³I. R. Shein, A. L. Ivanovskii, E. Z. Kurmaev, A. Moewes, S. Chiuzbian, L. D. Finkelstein, M. Neumann, Z. A. Ren, and G. C. Che, *Phys. Rev. B* **66**, 024520 (2002).

⁴J. H. Kim, J. S. Ahn, J. Kim, M.-S. Park, S. I. Lee, E. J. Choi, and S.-J. Oh, *Phys. Rev. B* **66**, 172507 (2002).

⁵C. Sulkowski, T. Klimczuk, R. J. Cava, and K. Rogacki, *Phys. Rev. B* **76**, 060501(R) (2007), and references therein.

⁶P. M. Singer, T. Imai, T. He, M. A. Hayward, and R. J. Cava, *Phys. Rev. Lett.* **87**, 257601 (2001).

⁷D. P. Young, M. Moldovan, and P. W. Adams, *Phys. Rev. B* **70**, 064508 (2004).

⁸Z. Q. Mao, M. M. Rosario, K. D. Nelson, K. Wu, I. G. Deac, P. Schiffer, Y. Liu, T. He, K. A. Regan, and R. J. Cava, *Phys. Rev. B* **67**, 094502 (2003).

⁹R. Prozorov, A. Snezhko, T. He, and R. J. Cava, *Phys. Rev. B* **68**, 180502 (2003).

¹⁰J.-Y. Lin, P. L. Ho, H. L. Huang, P. H. Lin, Y.-L. Zhang, R.-C. Yu, C.-Q. Jin, and H. D. Yang, *Phys. Rev. B* **67**, 052501 (2003).

¹¹L. Shan, K. Xia, Z. Y. Liu, H. H. Wen, Z. A. Ren, G. C. Che, and Z. X. Zhao, *Phys. Rev. B* **68**, 024523 (2003).

¹²A. Wälte, G. Fuchs, K.-H. Müller, A. Handstein, K. Nenkov, V. N. Narozhnyi, S.-L. Drechsler, S. Shulga, L. Schultz, and H. Rosner, *Phys. Rev. B* **70**, 174503 (2004).

- ¹³L. Shan, Z. Y. Liu, Z. A. Ren, G. C. Che, and H. H. Wen, *Phys. Rev. B* **71**, 144516 (2005).
- ¹⁴L. Shan, H. J. Tao, H. Gao, Z. Z. Li, Z. A. Ren, G. C. Che, and H. H. Wen, *Phys. Rev. B* **68**, 144510 (2003).
- ¹⁵H. S. Lee, D. J. Jang, H. G. Lee, S. I. Lee, S. M. Choi, and C. J. Kim, *Adv. Mater.* **19**, 1807 (2007).
- ¹⁶P. Diener, P. Rodière, T. Klein, C. Marcenat, J. Kacmarcik, Z. Pribulova, D. J. Jang, H. S. Lee, H. G. Lee, and S. I. Lee, *Phys. Rev. B* **79**, 220508(R) (2009).
- ¹⁷P. F. Sullivan and G. Seidel, *Phys. Rev.* **173**, B679 (1968).
- ¹⁸J. Kacmarcik, Z. Pribulová, C. Marcenat, T. Klein, P. Rodière, L. Cario, and P. Samuely, *Phys. Rev. B* **82**, 014518 (2010).
- ¹⁹R. Heid, B. Renker, H. Schober, P. Adelman, D. Ernst, and K.-P. Bohnen, *Phys. Rev. B* **69**, 092511 (2004).
- ²⁰H. Padamsee, J. E. Neighbor, and C. A. Shiffman, *J. Low Temp. Phys.* **12**, 387 (1973).
- ²¹A. M. Toxen, *Phys. Rev. Lett.* **15**, 462 (1965).
- ²²E. H. Brandt, *Phys. Rev. B* **68**, 054506 (2003).
- ²³N. R. Werthamer, E. Helfand, and P. C. Hohenberg, *Phys. Rev.* **147**, 295 (1966).
- ²⁴A. M. Clogston, *Phys. Rev. Lett.* **9**, 266 (1962).
- ²⁵N. R. Werthamer and W. L. McMillan, *Phys. Rev.* **158**, 415 (1967).
- ²⁶S. V. Shulga and S.-L. Drechsler, *J. Low Temp. Phys.* **129**, 93 (2002).
- ²⁷H.-S. Lee, D.-J. Jang, H.-G. Lee, W. Kang, M. H. Cho, and S. I. Lee, *J. Phys. Condens. Matter* **20**, 255222 (2008).
- ²⁸T. Klein, D. Braithwaite, A. Demuer, W. Knafo, G. Lapertot, C. Marcenat, P. Rodiere, I. Sheikin, P. Strobel, A. Sulpice, and P. Toulemonde, *Phys. Rev. B* **82**, 184506 (2010).
- ²⁹A. Tamai, A. Y. Ganin, E. Rozbicki, J. Bacsá, W. Meevasana, P. D. C. King, M. Caffio, R. Schaub, S. Margadonna, K. Prassides, M. J. Rosseinsky, and F. Baumberger, *Phys. Rev. Lett.* **104**, 097002 (2010).
- ³⁰A. Pleceník, M. Grajcar, S. Benacka, P. Seidel, and A. Pfuch, *Phys. Rev. B* **49**, 10016 (1994).
- ³¹Remarkably, from the fits to the low-temperature $\lambda(T)$ measurements probing ≈ 100 nm below surface, the energy gap around 1 meV has been determined.¹⁶
- ³²P. Szabó, P. Samuely, Z. Pribulová, M. Angst, S. Bud'ko, P. C. Canfield, and J. Marcus, *Phys. Rev. B* **75**, 144507 (2007).